

Toward Metal-Mediated C–F Bond Formation. Synthesis and Reactivity of the 16-Electron Fluoro Complex [RuF(dppp)₂]PF₆ (dppp = 1,3-Bis(diphenylphosphino)propane)

Peter Barthazy, Robert M. Stoop, Michael Wörle,[†] Antonio Togni,* and Antonio Mezzetti*

Laboratory of Inorganic Chemistry, Swiss Federal Institute of Technology, ETH Zentrum, CH-8092 Zürich, Switzerland

Received January 7, 2000

The five-coordinate fluoro complex [RuF(dppp)₂]PF₆ (**1a**) has been prepared by reacting [RuCl(dppp)₂]PF₆ (**1b**) with TlF (dppp = 1,3-bis(diphenylphosphino)propane). An X-ray investigation of **1a** shows a distorted trigonal bipyramidal geometry (Y-shaped). The 16-electron complex **1a** reacts with a number of donors, including CO, H₂, and F⁻. The X-ray structure of *trans*-[RuF(CO)(dppp)₂]PF₆ (**2aBPh₄**) suggests that the π -donor ability of the fluoro ligand is only slightly higher than that of chloride. The reaction of **1a** with [Me₄N]F gives *cis*-[RuF₂(dppp)₂] (**3**), a rare difluoro complex not stabilized by π -acidic co-ligands. The Ru–F bond of **1a** is hydrogenolyzed upon reaction with H₂ to give [RuH(η^2 -H₂)(dppp)₂]⁺. The coordinatively unsaturated complex **1a** reacts with activated haloalkanes R–X (X = Cl or Br) in 1:1 molar ratio to give the fluorinated organic derivative and [RuX(dppp)₂]⁺. The halide metathesis proceeds instantaneously and quantitatively with (*E*)-3-bromo-1,3-diphenylpropene and chlorotriphenylmethane. Substrate conversion decreases with decreasing substitution at the halogen-bearing carbon atom.

Introduction

Selective and efficient carbon–fluorine bond-forming reactions evoke great interest in modern synthetic chemistry, due to the importance of fluororganic compounds both in medicinal chemistry and biochemistry.¹ Whereas in recent years many fluorinating agents have been developed, the use of transition metal complexes has been very much focused on carbon–fluorine bond-breaking processes.^{2–6} In contrast, investigations of selective C–F bond formation are mainly restricted to fluoroacyl complexes⁷ and to the use of low-valent

fluoride salts⁸ or high-valent metal fluorides and oxofluorides.⁹ Although low-valent fluoro complexes of transition metals have long been known to react with halogenated solvents,¹⁰ it has been shown only recently that fluorinated organic products are formed thereby.¹¹ Furthermore, coordination chemical aspects of fluorine chemistry have constituted the object of systematic

* E-mail: mezzetti@inorg.chem.ethz.ch, togni@inorg.chem.ethz.ch.

[†] X-ray structures of complexes **1a**, **2a**, and **3**.

(1) See, for example: (a) Methods of Organic Chemistry (Houben-Weyl), *Organo-Fluorine Compounds*; Baasner, B.; Hagemann, H., Tatlow, J. C., Eds.; Thieme Verlag: Stuttgart, 1999; Vol. E10a, and references therein. (b) ACS Monograph 187, *Chemistry of Organic Fluorine Compounds II*; Hudlicky, M.; Pavlath, A. E., Eds.; American Chemical Society: Washington, DC, 1995. (c) Wilkinson, J. A. *Chem. Rev.* **1992**, *92*, 505. (d) *Selective Fluorination in Organic and Bioinorganic Chemistry*; Welch, T. J., Ed.; ACS Symposium Series 456; American Chemical Society: Washington, DC, 1990.

(2) Kiplinger, J. L.; Richmond, T. G.; Osterberg, C. E. *Chem. Rev.* **1994**, *94*, 373.

(3) Burdeniuc, J.; Siegbahn, P. E.; Crabtree, R. H. *New J. Chem.* **1998**, *503*. Burdeniuc, J.; Jedlicka, B.; Crabtree, R. H. *Chem. Ber./Recl.* **1997**, *130*, 145.

(4) Braun, T.; Parsons, S.; Perutz, R. N.; Voith, M. *Organometallics* **1999**, *18*, 1710. Cronin, L.; Higgitt, C. L.; Karch, R.; Perutz, R. N. *Organometallics* **1997**, *16*, 4920.

(5) Aizenberg, M.; Milstein, D. *Science* **1994**, *265*, 359. Aizenberg, M.; Milstein, D. *J. Am. Chem. Soc.* **1995**, *117*, 9674.

(6) Kiplinger, J. L.; Richmond, T. G. *J. Chem. Soc., Chem. Commun.* **1996**, *1115*; *J. Am. Chem. Soc.* **1996**, *118*, 1805.

(7) (a) Brewer, S. A.; Coleman, K. S.; Fawcett, J.; Holloway, J. H.; Hope, E. G.; Russell, D. R.; Watson, P. G. *J. Chem. Soc., Dalton Trans.* **1995**, 1073. (b) Blake, A. J.; Cockman, R. W.; Ebsworth, E. A. V.; Holloway, J. H. *J. Chem. Soc., Chem. Commun.* **1988**, 529.

(8) Taverner, S. J.; Heath, P. A.; Clark, J. H. *New J. Chem.* **1998**, 655, and references therein.

(9) (a) Dukat, W. W.; Holloway, J. H.; Hope, E. G.; Rieland, M. R.; Townson, P. J.; Powell, R. L. *J. Chem. Soc., Chem. Commun.* **1993**, 1429. (b) Holloway, J. H.; Hope, E. G.; Townson, P. J.; Powell, R. L. *J. Fluorine Chem.* **1996**, *76*, 105.

(10) (a) Kemmitt, R. D. W.; Peacock, R. D.; Stocks, J. J. *J. Chem. Soc., Dalton Trans.* **1975**, 1159.

(11) Fraser, S. L.; Antipin, M. Y.; Khroustlyov, V. N.; Grushin, V. V. *J. Am. Chem. Soc.* **1997**, *119*, 4769. Pilon, M. C.; Grushin, V. V. *Organometallics* **1998**, *17*, 1774. Grushin, V. V. *Angew. Chem., Int. Ed.* **1998**, *37*, 994.

(12) Review articles: (a) Murphy, E. F.; Murugavel, R.; Roesky, H. W. *Chem. Rev.* **1997**, *97*, 3425. (b) Doherty, N. M.; Hoffman, N. W. *Chem. Rev.* **1991**, *91*, 553.

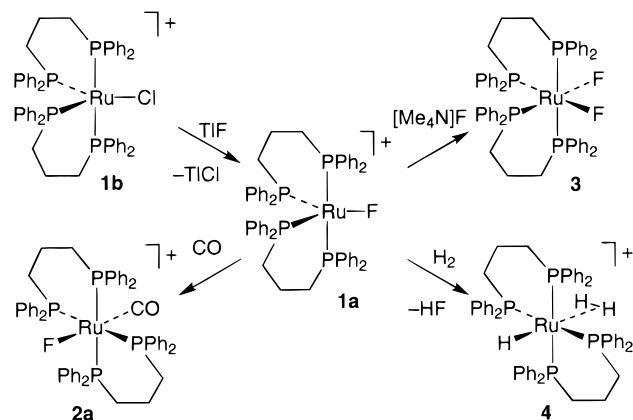
(13) (a) Poulton, J. T.; Sigalas, M. P.; Eisenstein, O.; Caulton, K. G. *Inorg. Chem.* **1993**, *32*, 5490. (b) Poulton, J. T.; Sigalas, M. P.; Foltling, K.; Streib, W.; Eisenstein, O.; Caulton, K. G. *Inorg. Chem.* **1994**, *33*, 1476. (c) Cooper, A. C.; Foltling, K.; Huffman, J. C.; Caulton, K. G. *Organometallics* **1997**, *16*, 505. (d) Ogasawara, M.; Huang, D.; Streib, W. E.; Huffman, J. C.; Gallego-Planas, N.; Maseras, F.; Eisenstein, O.; Caulton, K. G. *J. Am. Chem. Soc.* **1997**, *119*, 8642.

(14) Veltheer, J. E.; Burger, P.; Bergman, R. G. *J. Am. Chem. Soc.* **1995**, *117*, 12478.

(15) Whittlesley, M. K.; Perutz, R. N.; Greener, B.; Moore, M. H. *Chem. Commun.* **1997**, 187.

(16) (a) Coleman, K. S.; Fawcett, J.; Holloway, J. H.; Hope, E. G.; Russell, D. R. *J. Chem. Soc., Dalton Trans.* **1997**, 3557. (b) Cockman, R. W.; Ebsworth, E. A. V.; Holloway, J. H.; Murdoch, H.; Robertson, N.; Watson, P. G. In *Inorganic Fluorine Chemistry*; Thrasher, J. S., Strauss, S. H., Eds.; ACS Symposium Series 555; American Chemical Society: Washington, DC, 1994.

Scheme 1



studies only recently.^{12–17} In this context, we are engaged in a fundamental study directed toward the development of metal-mediated or metal-catalyzed fluorination reactions. Clearly, to this goal a deeper knowledge of the coordination chemistry of fluoride is required.

The π -donating ability of fluoride is found to stabilize complexes of the early or middle transition metals.¹² On the other hand, the same effect explains the relative instability of coordinatively saturated late transition metal fluoro complexes, unless strong π -accepting ligands are present. Thus, the π -donor fluoride is an excellent candidate for stabilizing 16-electron complexes such as $[\text{MX}(\text{P}-\text{P})_2]^{n+}$ ($\text{M} = \text{d}^6$ metal center, $\text{X} = \text{F}$).^{18,19} The latter species adopts a distorted trigonal-bipyramidal (Y-shaped) structure in order to optimize the $\text{X} \rightarrow \text{M}$ π -donation ($\text{X} = \text{Cl}$).¹⁸ However, five-coordinate fluoro complexes with a 16-electron count are extremely rare.¹³ Furthermore, many of the reported fluoro phosphine complexes are stabilized by strong π -acid co-ligands, typically CO.^{7a,13,16,17}

We report herein the synthesis and X-ray structures of $[\text{RuF}(\text{dppp})_2]^+$ (**1a**) and *cis*- $[\text{RuF}_2(\text{dppp})_2]$ (**3**), containing the very rare FP_4 and F_2P_4 donor sets,^{16b} respectively. Furthermore, we present the use of derivative **1a** as a fluorinating agent for organic molecules containing activated carbon–halide bonds. Part of this work has appeared as a preliminary communication.²⁰

Results and Discussion

$[\text{RuF}(\text{dppp})_2]\text{PF}_6$ (1a**).** The five-coordinate species $[\text{RuCl}(\text{dppp})_2]\text{PF}_6$ (**1b**)^{19a} reacts with TlF giving the red fluoro analogue $[\text{RuF}(\text{dppp})_2]\text{PF}_6$ (**1a**) (Scheme 1). The driving force for this metathesis reaction is the low solubility of TlCl. Similarly to the chloro analogue **1b**, **1a** exhibits a static ³¹P spectrum (AA'MM' part of a

Table 1. Selected Bond Distances (Å) and Angles (deg) for $[\text{RuF}(\text{dppp})_2]\text{PF}_6$ (**1a**)

| | | | |
|---------------|-----------|---------------|----------|
| Ru–F(1A) | 2.030(7) | Ru–F(1B) | 2.033(9) |
| Ru–P(1) | 2.423(1) | Ru–P(3) | 2.408(1) |
| Ru–P(2) | 2.261(1) | Ru–P(4) | 2.254(1) |
| F(1A)–Ru–P(1) | 88.8(2) | F(1B)–Ru–P(1) | 85.8(2) |
| F(1A)–Ru–P(2) | 125.3(2) | F(1B)–Ru–P(2) | 145.5(2) |
| F(1A)–Ru–P(3) | 82.9(2) | F(1B)–Ru–P(3) | 85.5(2) |
| F(1A)–Ru–P(4) | 139.6(2) | F(1B)–Ru–P(4) | 119.7(2) |
| P(1)–Ru–P(2) | 89.41(4) | P(2)–Ru–P(3) | 97.40(4) |
| P(1)–Ru–P(3) | 171.26(4) | P(2)–Ru–P(4) | 94.85(4) |
| P(1)–Ru–P(4) | 96.51(4) | P(3)–Ru–P(4) | 88.39(4) |

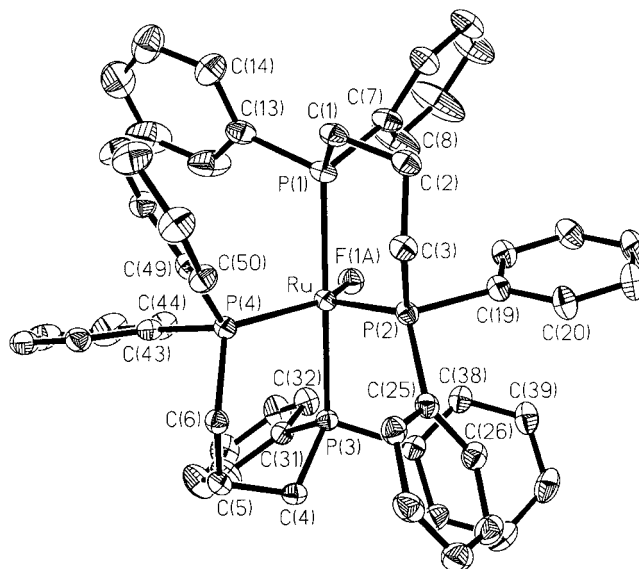


Figure 1. ORTEP view of $[\text{RuF}(\text{dppp})_2]\text{PF}_6$ (**1a**) (30% probability ellipsoids, only F(1A) is shown).

AA'MM'X spin system, CD_2Cl_2), which confirms the presence of the fluoro ligand. The high-frequency doublet of triplets at δ 49.0 is attributed to the equatorial P atoms. The fluoride ligand is more strongly coupled to the equatorial ($J_{\text{P,F}} = 47.1$ Hz) than to the axial P atoms at δ -7.1 ($J_{\text{P,F}} = 15.2$ Hz). The ¹⁹F NMR spectrum features the fluoro ligand as a triplet of triplets (X part of AA'MM'X) at δ -203.4 with the same coupling constants observed in the ³¹P NMR spectrum. As already observed for a number of fluoro complexes,¹¹ the P,F coupling is not observed in CDCl_3 containing traces of water. Addition of activated molecular sieves to the NMR samples in moist CDCl_3 gives well-resolved ³¹P and ¹⁹F NMR spectra. The Ru–F stretching mode of **1a** could not be identified in the IR spectrum.

The X-ray structure of $[\text{RuF}(\text{dppp})_2]\text{PF}_6$ has been determined, and selected interatomic distances and angles are listed in Table 1. The metric data of cation $[\text{RuF}(\text{dppp})_2]^+$ are very similar to those of the chloro analogue **1b**.²¹ As expected for a π -stabilized 16-electron complex,¹⁸ the equatorial plane shows a large deviation away from the ideal trigonal-bipyramidal geometry, with the P(2)–Ru–P(4) closed down to 94.85(4)° (Figure 1). As already observed in related species,^{18,19} the Y-shaped coordination is further distorted, with unequal F–Ru–P_{eq} angles (Table 1). Both chelate rings have a flattened chair conformation. The fluoride ligand is disordered between two positions (F(1A) and F(1B), at

(17) Ilg, K.; Werner, H. *Organometallics* **1999**, *18*, 5426.

(18) (a) Caulton, K. G. *New J. Chem.* **1994**, *18*, 25. (b) Riehl, J.-F.; Jean, Y.; Eisenstein, O.; Péliissier, M. *Organometallics* **1992**, *11*, 729. (c) Johnson, T. J.; Folting, K.; Streib, W. E.; Martin, J. D.; Huffman, J. C.; Jackson, S. A.; Eisenstein, O.; Caulton, K. G. *Inorg. Chem.* **1995**, *34*, 488, and references therein.

(19) See for instance: (a) Bressan, M.; Rigo, P. *Inorg. Chem.* **1975**, *14*, 2286. (b) Mezzetti, A.; Del Zotto, A.; Rigo, P.; Bresciani Pahor, N. *J. Chem. Soc., Dalton Trans.* **1989**, 1045. (c) Chin, B.; Lough, A. J.; Morris, R. H.; Schweitzer, C. T.; D'Agostino, C. *Inorg. Chem.* **1994**, *33*, 6278. (d) de los Rios, I.; Jiménez-Tenorio, M.; Puerta, M. C.; Salcedo, I.; Valerga, P. *J. Chem. Soc., Dalton Trans.* **1997**, 4619.

(20) Barthazy, P.; Hintermann, L.; Stoop, R. M.; Wörle, M.; Mezzetti, A.; Togni, A. *Helv. Chim. Acta* **1999**, *82*, 2448.

(21) Batista, A. A.; Centeno Cordeiro, L. A.; Oliva, G. *Inorg. Chim. Acta* **1993**, *203*, 185.

0.728(9) Å from each other) approximately lying in the equatorial plane. Resolved electron density maxima for the disordered halide ligand were obtained in the Fourier map from diffraction data collected at -60°C .²² The similar occupancies of the two F sites (46 and 40% for F(1A) and F(1B), respectively) suggest similar energies for both positions. A minor electron density peak is interpreted as isomorphous substitution of F with Cl (14% of total), which is apparently due to partial F/Cl exchange during crystallization, as confirmed by ^{31}P NMR.²³ The Ru–Cl distance (2.315(11) Å) is close to the value found in **1b** (2.371(5) Å).²¹

Analysis of the nonbonded contacts reveals that the positional disorder maximizes the F \cdots H hydrogen bonds to the six phenyl rings forming a pocket around the halide ligand in both **1a** and **1b**. Comparison of the X-ray structures of **1b** and **1a** shows that, on going from Cl to F, a twist of the axial phenyls C(7)–C(12) and C(31)–C(36) reduces the nonbonded distances between the ortho H atoms and X (X = Cl and F, respectively) from values in the range 2.49–2.99 Å in **1b** to 2.17–2.59 Å in **1a**. As will be discussed below, other fluoro complexes exhibit nonbonded F \cdots H distances significantly shorter than the sum of the van der Waals radii (2.67 Å).¹⁶ The P(1)–Ru–P(3) angle between the trans P_{ax} atoms is closed down to $171.26(4)^{\circ}$, probably as an effect of both the steric crowding due to the large bite angle of dppp (close to 90°) and the attractive F \cdots H interaction.

The Ru–F distance deserves particular attention as a diagnostic tool for the extent of the π -donation. Unfortunately, large standard deviations are associated with the positional parameters of F(1A) and F(1B) due to partial overlap of their electron densities, and caution is required in discussing the Ru–F bond distances (2.030(7) and 2.033(9) Å, respectively). Taking as reference the Ru–Cl distance of 2.371(5) Å in **1b**,²¹ a calculated value of 2.02 Å is obtained by subtracting the difference of the atomic radii of F and Cl (0.35 Å). The closeness of observed and calculated values suggests that the π -contribution to the bonding is similar in **1a** and **1b**. The Ru–P distances are very similar to those of **1b**, with Ru– P_{ax} much longer than Ru– P_{eq} . This is expected on the basis of trans influence effects and is reflected in the ^{31}P NMR shifts (see above).

[RuF(CO)(dppp)₂]PF₆ (2aPF₆). In agreement with its unsaturated nature, complex **1a** reacts with a number of donors. The reaction with CO is instantaneous in CH_2Cl_2 , and yields *trans*-[RuF(CO)(dppp)₂]PF₆ (**2aPF₆**) (Scheme 1).²⁴ Complex **2aPF₆** features a broad singlet at δ 3.0 in the ^{31}P NMR spectrum. Similarly broadened signals have been previously observed for the related six-coordinate complexes *trans*-[RuCl(η^2 -H₂)-(dppp)₂]⁺²⁵ and are probably due to the inversion at ruthenium in the tetrahedrally distorted RuP₄ plane

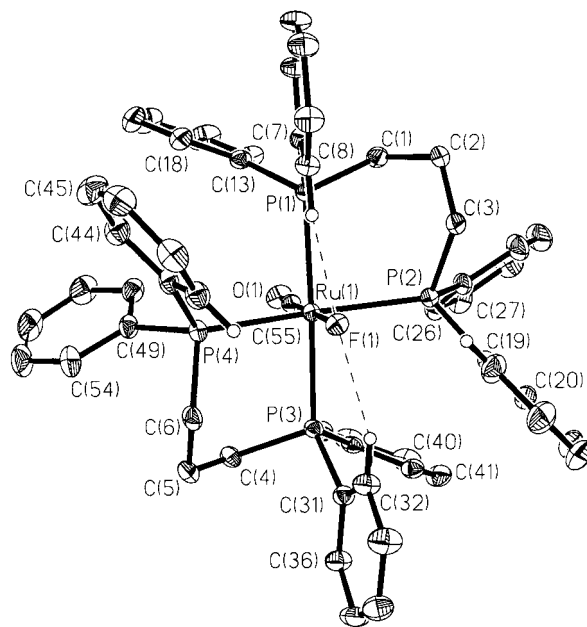


Figure 2. ORTEP view of [RuF(CO)(dppp)₂]BPh₄ (**2a**) (30% probability ellipsoids).

Table 2. Selected Interatomic Distances (Å) and Angles (deg) for [RuF(CO)(dppp)₂]PF₆ (**2a**)

| | | | |
|---------------------|----------|---------------------|-----------|
| Ru–F(1) | 2.069(2) | Ru–C(55) | 1.830(4) |
| Ru–P(1) | 2.433(1) | Ru–P(3) | 2.434(1) |
| Ru–P(2) | 2.424(1) | Ru–P(4) | 2.426(1) |
| C(55)–O(1) | 1.152(5) | | |
| F(1) \cdots H(8) | 2.29 | F(1) \cdots H(24) | 2.52 |
| F(1) \cdots H(32) | 2.29 | F(1) \cdots H(48) | 2.51 |
| F(1)–Ru–C(55) | 179.7(1) | C(55)–Ru–P(4) | 97.8(1) |
| F(1)–Ru–P(1) | 95.67(7) | P(1)–Ru–P(2) | 86.07(4) |
| F(1)–Ru–P(2) | 81.61(7) | P(1)–Ru–P(3) | 170.13(4) |
| F(1)–Ru–P(3) | 94.20(7) | P(1)–Ru–P(4) | 95.19(4) |
| F(1)–Ru–P(4) | 82.35(7) | P(2)–Ru–P(3) | 95.15(4) |
| C(55)–Ru–P(1) | 84.6(1) | P(2)–Ru–P(4) | 163.96(4) |
| C(55)–Ru–P(2) | 98.2(1) | P(3)–Ru–P(4) | 86.36(4) |
| C(55)–Ru–P(3) | 85.5(1) | | |

caused by the large bite angle of the dppp ligand (see below). In the ^{19}F NMR spectrum, a broad singlet at δ -401 confirms the presence of the fluoro ligand.

The $\nu(\text{CO})$ stretching frequency of **2aPF₆** (1944 cm^{-1} , KBr) is lower than that of the chloro analogue [RuCl(CO)(dppp)₂] (**2b**)^{19a} (1953 cm^{-1} , KBr). This follows the trend observed for other complexes containing an X–M–CO fragment (X = halide), which has been explained by assuming that fluoride is a better π -donor than its heavier analogues.^{12b,16} Also, it has been argued that the lone pairs of the fluoride ligands destabilize the metal orbitals having the appropriate π -symmetry (d_{xz} and d_{yz} assuming the F–Ru–CO vector as the z axis). This four-electron repulsion is larger with fluoride than with the heavier halides, which enhances the π -backdonation to the carbonyl ligand (push–pull interaction) in the fluoro analogue.^{18a} To get further insight into these effects, we have determined the X-ray structure of the tetraphenylborate salt **2aBPh₄**.

The [RuF(CO)(dppp)₂]⁺ cation has a distorted octahedral geometry with pseudo- C_2 symmetry (Figure 2, Table 2). The trans P–Ru–P angles ($170.13(4)^{\circ}$ and $163.96(4)^{\circ}$) deviate largely from the ideal value, resulting in a tetrahedral distortion of the P₄ plane: P(1) and P(3) are off the mean plane by 0.275 and 0.274 Å, and P(2) and P(4) by 0.275 and 0.274 Å on the opposite side.

(22) At room temperature the maxima are not resolved.

(23) In view of the reactivity of **1a** with alkyl halides, the F/Cl exchange is apparently not due to the reaction of **1a** with CH_2Cl_2 , but rather to traces of HCl (see below). Attempts at growing suitable crystals in other solvents were unsuccessful.

(24) (a) There is no evidence of the formation of the cis isomer as intermediate.^{24b} (b) Mezzetti, A.; Del Zotto, A.; Rigo, P. *J. Chem. Soc., Dalton Trans.* **1990**, 2515.

(25) Rocchini, E.; Mezzetti, A.; Rügger, H.; Burckhardt, U.; Gramlich, V.; Del Zotto, A.; Martinuzzi, P.; Rigo, P. *Inorg. Chem.* **1997**, *36*, 711.

Table 3. Selected IR and X-ray Data for **2a**, **2c**, and $[\text{RuF}_2(\text{CO})_2(\text{PPh}_3)_2]$

| | $[\text{RuF}(\text{CO})(\text{dppp})_2]^+$ (2a) | $[\text{RuCl}(\text{CO})(\text{dppm})_2]^+$ (2c) ^a | $[\text{RuF}_2(\text{CO})_2(\text{PPh}_3)_2]^b$ |
|-------------------------------------|---|---|---|
| $\nu(\text{CO})$, cm^{-1} | 1944 ^c | 1973 ^d | 2045, 1973 ^d |
| $d(\text{Ru}-\text{X})$, Å | 2.069(2) | 2.422(3) | 2.011(4) |
| $d(\text{Ru}-\text{C})$, Å | 1.830(4) | 1.849(9) | 1.841(7) |
| $d(\text{C}-\text{O})$, Å | 1.152(5) | 1.11(1) | 1.135(9) |

^a From ref 26. ^b From ref 16a. ^c In KBr. ^d In Nujol.

This is apparently due to steric crowding, as indicated by the twist conformation of the chelate rings. Two phenyl rings are involved in short nonbonded distances between the fluoro ligand and the ortho H atoms H(8) and H(32) (2.29 Å, Table 2). As the covalent radius of ruthenium remains nearly constant on going from five-coordinate **1a** to six-coordinate **2a** (the Ru–P distances involving mutually trans phosphines increase by only ca. 0.01 Å), the Ru–F distances in **1a** and **2a** (2.03 and 2.07 Å, respectively) suggest that the F → Ru π -bonding is stronger in the former complex. The experimental Ru–F distance in **2a** is identical to the value calculated by subtracting the difference between the covalent radii of Cl and F (0.35 Å) from the Ru–Cl distance in the closely related chloro carbonyl complex $[\text{RuCl}(\text{CO})(\text{dppm})_2]^+$ (**2c**, dppm = bis(diphenylphosphino)methane) (2.42 Å).²⁶ This would suggest that both the fluoro carbonyl **2a** and the chloro analogue **2c** feature push–pull interactions of comparable magnitude, whereas comparison of the Ru–C (and C–O) distances suggests that metal-to-carbonyl back-bonding is stronger in the case of the fluoro derivative **2a** (Table 3).²⁷

Comparison with complexes of the type *cis,cis,trans*- $[\text{RuF}_2(\text{CO})_2(\text{PPh}_3)_2]$ ¹⁶ is less useful due to the different charge of the complex (0 vs +1) and to the different donor sets ($\text{F}_2(\text{CO})_2\text{P}_2$ vs $\text{F}(\text{CO})\text{P}_4$). The data in Table 3 indicate a higher degree of Ru → CO π -back-donation (but a weaker F → Ru π -bond) in **2a** than in $[\text{RuF}_2(\text{CO})_2(\text{PPh}_3)_2]$. This suggests that the presence of a second carbonyl ligand in $[\text{RuF}_2(\text{CO})_2(\text{PPh}_3)_2]$ enhances the competition for the d_{π} -electrons of ruthenium, leading to a lower Ru–C bond order (and higher Ru–F bond order) than in **2a**.

$[\text{RuF}_2(\text{dppp})_2]$ (3**).** Complex **1a** reacts with $[\text{Me}_4\text{N}]\text{F}$ (1.8 equiv) in CH_2Cl_2 giving *cis*- $[\text{RuF}_2(\text{dppp})_2]$ (**3**) (Scheme 1). Complex **3** is a rare example of a six-coordinate difluoro complex of a d^6 metal center that does not contain strong π -acceptor ligands, such as CO.^{16b} The ³¹P and ¹⁹F NMR spectral pattern of **3** (AA'MM'XX' spin system) is indicative of a *cis* configuration (Figure 3). The AA' part at δ 30.9 is attributed to the P atoms trans to F, and the mutually trans P atoms (MM') show their resonance at δ 1.3. The ¹⁹F NMR spectrum features the fluoro ligands (XX' part of AA'MM'XX') at δ –341.6. Simulation of both ³¹P and ¹⁹F NMR spectra yielded the chemical shifts and coupling constants (Figure 3). Two bands of medium intensity at 443 and 414 cm^{-1} in the

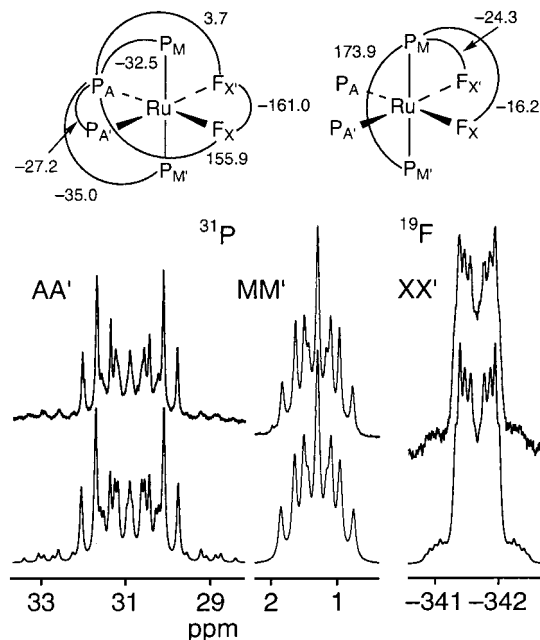


Figure 3. Experimental (above) and simulated (below) ³¹P (AA', MM') and ¹⁹F (XX') NMR spectra of **3**.

Table 4. Selected Interatomic Distances (Å) and Angles (deg) for $[\text{RuF}_2(\text{dppp})_2]$ (**3**) (molecule 1)

| | | | |
|-----------------|-----------|-----------------|-----------|
| Ru(1)–F(1) | 2.069(3) | Ru(1)–F(2) | 2.056(3) |
| Ru(1)–P(1) | 2.399(2) | Ru(1)–P(2) | 2.310(2) |
| Ru(1)–P(3) | 2.389(2) | Ru(1)–P(4) | 2.303(2) |
| F(1)···H(18) | 2.09 | F(2)···H(24) | 2.08 |
| F(1)···H(44) | 2.12 | F(2)···H(38) | 2.07 |
| F(1)–Ru(1)–F(2) | 78.2(1) | F(2)–Ru(1)–P(1) | 87.1(1) |
| F(1)–Ru(1)–P(1) | 85.5(1) | F(2)–Ru(1)–P(2) | 92.90(9) |
| F(1)–Ru(1)–P(2) | 170.5(1) | F(2)–Ru(1)–P(3) | 85.3(1) |
| F(1)–Ru(1)–P(3) | 86.2(1) | F(2)–Ru(1)–P(4) | 171.00(9) |
| F(1)–Ru(1)–P(4) | 93.53(9) | P(2)–Ru(1)–P(3) | 96.32(6) |
| P(1)–Ru(1)–P(2) | 90.93(6) | P(2)–Ru(1)–P(4) | 95.57(6) |
| P(1)–Ru(1)–P(3) | 169.72(5) | P(3)–Ru(1)–P(4) | 90.75(6) |
| P(1)–Ru(1)–P(4) | 95.81(6) | | |

IR spectrum are attributed to the Ru–F stretching vibration.²⁸

Complex **3** has been studied by X-ray crystallography. The unit cell contains two crystallographically independent molecules, together with CH_2Cl_2 and hexane as solvent of crystallization. The structural parameters of the two independent molecules are essentially identical within standard deviations (Table 4). The coordination polyhedron is a distorted octahedron with mutually *cis* F atoms (Figure 4). The F–Ru–F angle is closed down to 78° as an effect of the steric bulk of the dppp ligands, which is also manifested in the *trans* P–Ru–P angle (ca. 170°). The conformation of both chelate rings is chair as in **1a**, whereas in **2a** both chelates have twist

(26) Szczepura, L. F.; Giambra, J.; See, R. F.; Lawson, H.; Janik, T. S.; Jircitano, A. J.; Churchill, M. R.; Takeuchi, K. J. *Inorg. Chim. Acta* **1995**, *239*, 77.

(27) The X-ray data of $[\text{RuCl}(\text{CO})(\text{dppe})_2]^+$ (dppe = 1,2-bis(diphenylphosphino)ethane), in which the Cl and CO ligands are disordered, are not discussed in view of the large errors of the Ru–Cl, Ru–C, and C–O distances.²⁶

(28) Nakamoto, K. *Infrared and Raman Spectra of Inorganic and Coordination Compounds*; Wiley: New York, 1995; Part B, p 265.

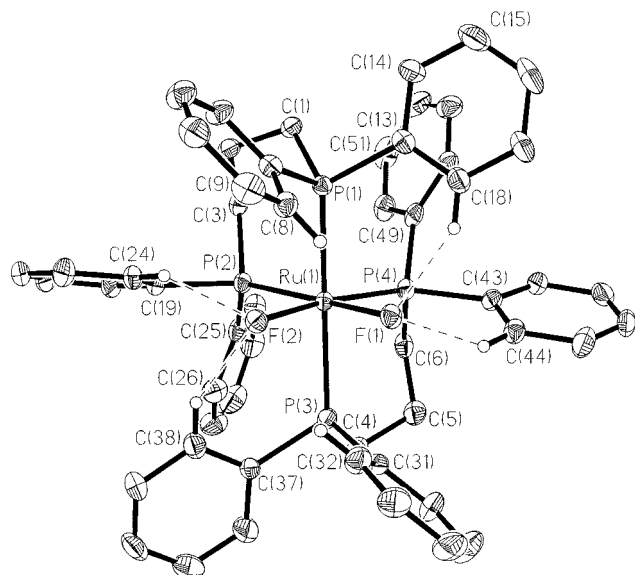


Figure 4. ORTEP view of *cis*-[RuF₂(dppp)₂] (**3**) (30% probability ellipsoids).

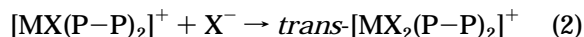
conformations, which is indicative of larger steric crowding. The Ru–F distances in **3** (average 2.06 Å) are significantly longer than in five-coordinate **1a** (average 2.03 Å) and slightly shorter than in **2a** (2.069(2) Å). The latter comparison suggests that the carbonyl ligand has a slightly larger trans influence toward the Ru–F bond than the phosphine. This contrasts with the trends observed for the trans influence toward the Ru–Cl bond in six-coordinate Ru(II) complexes.²⁹

Furthermore, four ortho H atoms of two axial and two equatorial phenyl rings of the first independent molecule are involved in short F···H contacts in the range 2.07–2.12 Å (the sum of the van der Waals radii is 2.67 Å) (Table 4, Figure 4).³⁰ The complexes [RuF₂(CO)₂-(PPh₃)₂] show similar features.^{16a,31} The fluoro ligands of the second independent molecule form four hydrogen bonds to phenyl H atoms (F···H distances between 2.07 and 2.12 Å) and one to a (non-disordered) CH₂Cl₂ molecule with a F(4)···H distance of 2.10 Å. The shortening of the H···F contacts on going from **1a** to **2a** and **3** reflects the increase both of the steric hindrance in the complexes and of the basicity of the F lone pairs (see below).

Complex **3** is more sensitive to traces of water than **1a** and must be protected from air moisture. Therefore, **3** was manipulated in a glovebox under purified nitrogen. In solution, exposure to traces of water leads to decomposition to unidentified products. Thus, the reactivity of the fluoro complexes on going from a 16-electron (**1a**) to an 18-electron complex (**3**) reflects the increase in the four-electron repulsion in this series. This shows that coordination to a metal fragment allows tuning the nucleophilic properties of the fluoride anion.

Finally, the stereochemistry of ligand attack onto five-coordinate **1a** to give the difluoro complex **3** deserves

some discussion. The stereochemical course of CO and halide addition to the related five-coordinate species [MX(dcpe)₂]⁺ (M = Ru or Os; X = Cl[−] or Br[−]; dcpe = 1,2-bis(dicyclohexylphosphino)ethane) has been studied as a function of the reaction temperature.^{24b} Below room temperature, both CO and halide ions give *cis* attack, in agreement with the P donor having a higher trans effect than halide. The resulting *cis*-[MX(L)(dcpe)₂]ⁿ⁺ (*n* = 1 or 0) adducts are stable at low temperature, but isomerize at room temperature, giving *trans*-[MX(L)(dcpe)₂]ⁿ⁺. When L is Cl[−] or Br[−], the isomerization reaction occurs by halide dissociation, followed by (slow) *trans* attack to give the kinetically inert *trans* isomer (eqs 1 and 2). In the case of the fluoro analogue **1a**, the



addition of the sixth ligand L apparently occurs with different stereochemistry depending on L, the attack being *trans* for L = CO and *cis* for L = F[−]. However, the *trans*-carbonyl adduct might be formed by fast isomerization of an initially formed, but undetected *cis* adduct. Accordingly, in the case of [RuCl(dcpe)₂]⁺, the initially formed *cis*-[RuCl(CO)(dcpe)₂]⁺ isomerizes at room temperature to give the thermodynamically stable and kinetically inert *trans*-[RuCl(CO)(dcpe)₂]⁺.^{24b} The preference for the *cis* attack is evident in the reaction of **1a** with F[−]. However, at difference with *cis*-[RuX₂(dcpe)₂] (X = Cl, Br),^{24b} the *cis*-difluoro complex **3** does not dissociate one fluoride at room temperature in CH₂Cl₂; that is, equilibrium 1 is completely shifted to the left when X is fluoride. An alternative explanation of the inability of **3** to undergo *cis*–*trans* isomerization might be related to the poor stability of the *trans* isomer caused by strong electron repulsion along the F–Ru–F axis.^{18a}

Reaction of [RuF(dppp)₂]⁺ with H₂. The five-coordinate chloro complexes [MCl(P–P)₂]⁺ (M = Ru, Os) are known to react with H₂ to give the elongated dihydrogen complexes [MCl(η²-H₂)(P–P)₂]⁺.^{25,32} In the case of the dppp derivative **1b**, the H₂-addition reaction is an equilibrium (*K* = 0.7 × 10^{−2} at 23 °C).²⁵ To investigate further the electronic effects of fluoride as compared to the other halides, we have studied the reaction of **1a** with H₂. Complex **1a** was dissolved in CDCl₃ in an NMR tube fitted with a Young valve, which was filled with H₂ (after evacuation) at room temperature. The solution color turns from red to yellow upon shaking the NMR tube in order to saturate the solvent with H₂. The ¹H and ³¹P NMR spectra of the reaction solution showed the signals of the already known [RuH(η²-H₂)(dppp)₂]⁺ (**4**).³³ A broad signal in the ¹⁹F NMR spectrum of the reaction mixture indicated that HF is formed.

(29) Brown, L. D.; Barnard, C. F. J.; Daniels, J. A.; Mawby, R. J.; Ibers, J. A. *Inorg. Chem.* **1978**, *17*, 2932.

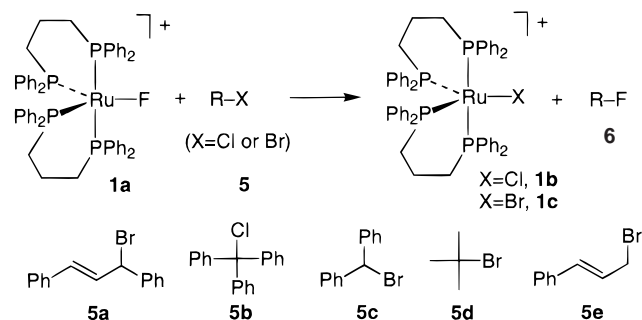
(30) The actual nonbonded distances are even shorter, as the F···H–C_{phenyl} distances are calculated assuming an apparent C–H distance of 0.93 Å.

(31) Intramolecular N–H···F bonds have been used to stabilize M(HF) complexes. See: Lee, D.-H.; Kwon, H. J.; Patel, B. P.; Liable-Sands, L. M.; Rheingold, A. L.; Crabtree, R. H. *Organometallics* **1999**, *18*, 1615.

(32) Cappellani, E. P.; Maltby, P. A.; Morris, R. H.; Schweitzer, C. T.; Steele, M. R. *Inorg. Chem.* **1989**, *28*, 4437. Mezzetti, A.; Del Zotto, A.; Rigo, P.; Farnetti, E. *J. Chem. Soc., Dalton Trans.* **1991**, 1525. Burrell, A. K.; Bryan, J. C.; Kubas, G. J. *J. Am. Chem. Soc.* **1994**, *116*, 1575. Chin, B.; Lough, A. J.; Morris, R. H.; Schweitzer, C. T.; D'Agostino, C. *Inorg. Chem.* **1994**, *33*, 6278. Maltby, P. A.; Schlaf, M.; Steinbeck, M.; Lough, A. J.; Morris, R. H.; Klooster, W. T.; Koetzle, T. F.; Srivastava, R. C. *J. Am. Chem. Soc.* **1996**, *118*, 5396.

(33) Saburi, M.; Aoyagi, K.; Takahashi, T.; Uchida, Y. *Chem. Lett.* **1990**, 601.

Scheme 2



Although the preparation of a fluoro dihydrogen complex seemed possible in view of the relative kinetic inertness of the Ru–F bond in these complexes, the reaction of **1a** with H₂ gives the hydrogenolysis product [RuH(η²-H₂)(dppp)₂]⁺ (**4**) (Scheme 1). This reaction is driven thermodynamically by the formation of HF and may involve an intermediate fluoro dihydrogen complex. It has been recently proposed³⁴ that the acidity of the putative dihydrogen complex [RuF(η²-H₂)(dppp)₂]⁺ should be close to that of [RuCl(η²-H₂)(dppp)₂]⁺ (pK_a is ca. 4).²⁵ Thus, the elimination of HF can be mediated by intramolecular proton transfer from the dihydrogen ligand to the more basic fluoride, followed by elimination. Also [RuH(F)(CO)(P^tBu₂Me)₂] has a labile Ru–F bond that is readily hydrogenolyzed.^{13a}

Fluorination Reactions. The fluoro ligand in complex **1a** can be transferred to activated organic electrophiles R–X (X = Br or Cl). The overall reaction is a halide metathesis that yields R–F and [RuX(dppp)₂]⁺ (Scheme 2). In a typical procedure, complex **1a** and the corresponding substrate **5a–e** (1 equiv) were dissolved in CDCl₃ in an NMR tube fitted with a Teflon liner and a Young valve. All manipulations were performed under purified nitrogen in a glovebox. The reaction was monitored by ¹H, ³¹P, and ¹⁹F NMR spectroscopy. The identity of the fluorinated products was determined by ¹⁹F NMR spectroscopy by comparison with literature data.^{20,35–38} Table 5 provides an overview of the reactions of **1a** with a number of alkyl bromides (or chloride) to give the corresponding fluorinated products. Conversion data are based on bromo derivative **5** and were determined as described below. The reaction of **5a** with **1a** occurs within seconds after mixing, as indicated by the immediate color change from red to brown. The ¹⁹F NMR spectrum of the reaction mixture shows that **6a** is the only fluorinated species besides [PF₆][–]. Integration of the ¹H NMR spectrum (see Experimental Section) indicates that **6a** is formed quantitatively (Table 5, run 1). The bromo derivative [RuBr(dppp)₂PF₆][–] (**1c**)^{19a} is the only complex present after completion of the reaction, as detected by ³¹P NMR spectroscopy. Also triphenylchloromethane **5b** reacts quantitatively to **6b**, as indicated by integration of the gate-decoupled ¹⁹F NMR

Table 5. Reactions of **1a** with R–X (**5a–e**)^a

| run | substrate | reaction time | conv (%) | selectivity (%) | ref ^b |
|-----|-----------|------------------|----------|-----------------|------------------|
| 1 | 5a | 1 min | 100 | 90 | 20 |
| 2 | 5b | 1 min | 100 | 100 | 35, 36 |
| 3 | 5c | 18 h | 70 | >90 | 36, 37 |
| 4 | 5d | 1 d ^c | 50 | 20 | 36, 38 |
| 5 | 5e | 1 d | 75 | ^d | |

^a Reaction conditions: **1a** (22 mg, 20 μmol) and 1 equiv of R–X (**5a–e**) (R = Br or Cl) were dissolved in CDCl₃ in a Teflon-coated NMR tube at room temperature (unless otherwise stated). Conversion is based on **5**, and selectivity is the percentage of converted **5** that forms **6a–d**. ^b Fluorinated products were identified by comparison of the ¹⁹F NMR data with literature values from cited papers. ^c At 50 °C. ^d Several unidentified products.

spectrum with the signal of the [PF₆][–] as reference (run 2). The ³¹P NMR spectrum shows that **1c** is formed quantitatively.

The reaction of **1a** with bromodiphenylmethane (**5c**) is much slower and not quantitative (run 3). The ¹H NMR spectrum of the reaction solution indicates that 70% of starting **5c** has reacted after 18-h reaction time at room temperature. The fluorinated product **6c** is formed with high selectivity, as shown by integration of the doublet at δ 6.48. The remaining converted substrate gives trace amounts of bis(diphenylmethyl) ether, as indicated by the ¹H NMR singlet at δ 5.40.³⁹ The gate-decoupled ¹⁹F NMR spectrum confirms that only **6c** contains fluorine. Integration of the spectrum with [PF₆][–] as reference is consistent with the yield of **6c** obtained from the ¹H NMR spectrum.

tert-Butyl bromide **5d** is even less reactive (50% conversion after 1 day at 50 °C, run 4) and gives lower selectivity to (CH₃)₃CF (20%), as determined by integration of the ¹H NMR spectrum. The main product is the elimination product isobutene (75% selectivity). A low-intensity singlet at δ 1.28 is attributed to (CH₃)₃COC-(CH₃)₃ (<5%) on the basis of its chemical shift⁴⁰ and by analogy with the reaction with **5a**, in which small amounts of the corresponding ether were detected.²⁰ Finally, (*E*)-3-bromo-1-phenylpropene **5e** forms a number of yet unidentified fluorinated organic products. Under the same conditions, 3-bromopropene and 2-iodopropane do not react over longer reaction times (3–7 days) at temperatures between 20 and 50 °C.

The substrates tested show a clear reactivity trend. Substrate conversion increases with increasing substitution at the halogen-bearing carbon in the case of both phenyl and alkyl groups. Thus, Ph₃CBr (**5b**) is more reactive than Ph₂CHBr (**5c**). In the alkyl series, the reaction of *tert*-butyl bromide is fast, whereas 2-iodopropane is completely unreactive. Increasing the size of the conjugated system has a similar effect: 1,3-Diphenylallyl bromide (**5a**) is more reactive than **5e**, but 3-bromopropene does not react. The F/Cl exchange observed upon standing of **1a** in CH₂Cl₂ deserves a final comment. Since **1a** does not react with allyl bromide and 2-iodopropane, which are stronger electrophiles than CH₂Cl₂, it is probable that the chlorination is due to the presence of traces of HCl formed from the chlorinated solvent upon standing rather than to direct reaction with CH₂Cl₂. In contrast to five-coordinate **1a**, the *cis*-

(34) Xu, Z. T.; Bytheway, I.; Jia, G. C.; Lin, Z. Y. *Organometallics* **1999**, *18*, 1761.

(35) Cox, D. P.; Terpinski, J.; Lawrynowicz, W. *J. Org. Chem.* **1984**, *49*, 3216.

(36) Lai, C.; Kim, Y. I.; Wang, C. M.; Mallouk, T. E. *J. Org. Chem.* **1993**, *58*, 1393.

(37) York, C.; Surya Prakash, G. K.; Olah, G. A. *Tetrahedron* **1996**, *52*, 9.

(38) Olah, G. A.; Baker, E. B.; Evans, J. C.; Tolgyesi, W. S.; McIntyre, J. S.; Bastien, I. J. *J. Am. Chem. Soc.* **1964**, *86*, 1360.

(39) Mizuno, H.; Matsuda, M.; Iino, M. *J. Org. Chem.* **1981**, *46*, 520.

(40) King, J. F.; Lam, J. Y. L.; Dave, V. *J. Org. Chem.* **1995**, *60*, 2831.

difluoro complex **3** (formed in situ from **1a** and CsF) does not react with **5b**. Thus, coordinative unsaturation is apparently necessary in order to trigger halide metathesis. We tentatively suggest that **1a** acts as a Lewis acid toward the alkyl bromide **5**, as well as a donor of fluoride and bromide scavenger. Fluorine exchange reactions between fluoro complexes and alkyl halides are not new. The reaction of fluoro complexes of Pt and Pd with chlorinated solvents has been shown to give the corresponding chloro complex.^{10,11} However, the nature of the organic product has rarely been ascertained, and the synthetic potential of this reaction has not been explored yet. One recent example is [PdF(Ph)(PPh₃)₂], which forms a mixture of CH₂ClF and CH₂F₂ by reaction with CH₂Cl₂ within hours.^{11b} Although high-valent metal fluorides and oxofluorides have been used for similar transformations,⁹ the systematic use of well-defined, low-valent fluoro complexes of a transition metal for selective C–F bond formation reactions under mild conditions is unprecedented. We are exploring further applications of 16-electron fluoro complexes of ruthenium in organic synthesis.

Conclusion

A formally coordinatively unsaturated, 16-electron fluoro complex of a relatively soft metal ion, such as ruthenium(II), is a stable species that reacts with an activated organic bromide to form a C–F bond. Although not yet of practical significance, the use of fluoro complexes containing diphosphine ligands in fluorination reactions clearly allows the transport of fluoride ions in organic solvents and their reaction with organic halides under mild conditions and opens new ways for asymmetric C–F bond formation.

Experimental Section

General Comments. All operations were carried out under argon using standard Schlenk techniques. All reagents and solvents were Fluka puriss. grade or had comparable purity. Diphenylallyl bromide was prepared according to a literature procedure,⁴¹ and the fluoro analogue (*E*)-3-fluoro-1,3-diphenylpropene as previously described.²⁰ NMR spectra were recorded on Bruker Avance 250 (¹H, ³¹P) and 300 (¹⁹F) spectrometers. Chemical shifts δ are in ppm relative to internal SiMe₄ (¹H, ¹³C) and to external 85% H₃PO₄. ¹⁹F NMR spectra are referenced to CFCl₃. Simulations of the ³¹P and ¹⁹F NMR spectra of **3** were performed with the programs WINDAISEY and WIN-NMR (Bruker Spectrospin). The spin system was defined as AA'MM'XX' (³¹P part AA'MM', ¹⁹F part XX') assuming positive trans ²J coupling constants and negative cis ones. However, J_{A,X'} refined to a small positive value of 3.7 Hz. A line broadening of 7.5 Hz was used. Infrared spectra were recorded on a Perkin-Elmer Paragon 1000 FT/IR spectrophotometer. FAB mass spectra were measured by the analytical service of Laboratorium für Organische Chemie of the ETH Zürich on a ZAB VSEQ instrument.

[RuF(dppp)₂]PF₆ (1a). A CH₂Cl₂ solution (20 mL) of [RuCl(dppp)₂]PF₆ (817 mg, 0.74 mmol) and TlF (200 mg, 0.90 mmol) was stirred for 3 h at room temperature. TlCl was filtered off, and a second portion of TlF (100 mg, 0.45 mmol) was added. After 2 h the Tl salts were filtered off, PrⁱOH (50 mL) was added, and CH₂Cl₂ was removed under vacuum to yield a red precipitate. The presence of CH₂Cl₂ (0.5 mol per mol of **1a**)

was determined by integration of a one-pulse ¹H NMR spectrum. Yield: 725 mg (90%). ¹H NMR (CDCl₃): δ 7.82 (s, br, 8 H, PhH), 6.8–7.5 (m, 32 H, PhH), 2.62 (s, br, 4 H, PCH₂), 2.0–2.5 (m, 4 H, PCH₂), 1.58 (s, br, 4 H, CH₂). ³¹P NMR (CDCl₃): δ 49.0 (d × t, 2 P, Ru–P, J_{P,F} = 47.1 Hz, J_{P,P} = 31.9 Hz), –7.1 (t × d, 2 P, Ru–P, J_{P,F} = 15.2 Hz, J_{P,P} = 31.9 Hz), –143.1 (septet, J_{P,F} = 710 Hz, 1 P, PF₆). ¹⁹F NMR: δ –74.5 (d, 6 F, J_{P,F} = 710 Hz, PF₆), –203.6 (t × t, J_{P,F} = 47 Hz, J_{P,P} = 15 Hz, 1 F, RuF). MS (FAB⁺): *m/z* 945 ([M]⁺, 100%), 511 ([M – dppp]⁺, 35%). Anal. Calcd for C₅₄H₅₂F₇P₅Ru·0.5 CH₂Cl₂: C, 57.81; H, 4.72. Found: C, 57.81; H, 4.82.

[RuBr(dppp)₂]PF₆ (1c). As in ref 18a. Further data: ¹H NMR (CDCl₃): δ 7.8–7.9 (m, 4 H, PhH), 7.1–7.6 (m, 24 H, PhH), 6.8–7.0 (m, 8 H, PhH), 2.9–3.0 (m, 2 H, CH₂), 2.6–2.7 (m, 2 H, CH₂), 2.1–2.5 (m, 4 H, CH₂), 1.6–1.7 (m, 2 H, CH₂), 0.8–0.9 (m, 2 H, CH₂). ³¹P NMR: δ 43.5 (t, 2 P, J_{P,P} = 32 Hz), –4.4 (t, 2 P, J_{P,P} = 32 Hz), –143 (septet, J_{P,F} = 710 Hz, PF₆). MS (FAB⁺): *m/z* 1007 ([M + H]⁺, 100), 926 ([M – Br]⁺, 6), 511 ([Ru(dppp)]⁺, 5).

[RuF(CO)(dppp)₂]PF₆ (2aPF₆). Compound **1a** (27 mg, 0.025 mmol) was dissolved in CH₂Cl₂ (10 mL), and CO gas was bubbled through the solution for 2 h. After adding PrⁱOH (20 mL) and hexane (20 mL) to the colorless solution, CH₂Cl₂ was removed under vacuum. The resulting white powder was filtered off. The presence of CH₂Cl₂ (0.5 mol per mol of **2aPF₆**) was determined by integration of a one-pulse ¹H NMR spectrum. Yield: 20 mg (72%). ¹H NMR (CDCl₃): δ 7.60 (s, br, 8 H, PhH), 7.45 (t, 4 H, J_{H,H'} = 7.4 Hz, PhH), 7.17–7.32 (m, 20 H, PhH), 6.9–7.1 (m, 8 H, PhH), 2.6–2.8 (m, 4 H, PCH₂), 2.2–2.4 (m, 4 H, PCH₂), 1.9–2.2 (m, 2 H, CH₂), 1.4–1.6 (m, 2 H, CH₂). ³¹P NMR (CDCl₃): δ 3.0 (br, 4 P, RuP), –143.1 (septet, J_{P,F} = 710 Hz, 1 P, PF₆). ¹⁹F NMR: δ –74.5 (d, 6 F, J_{P,F} = 710 Hz, PF₆), –400.8 (s, br, 1 F, RuF). IR (KBr, cm^{–1}): 1944, ν (CO), 842, ν (P–F). MS (FAB⁺): *m/z* 973 ([M]⁺, 561 ([M – dppp]⁺), 511 ([Ru – dppp]⁺), 335 ([dppp – Ph]⁺). Anal. Calcd for C₅₅H₅₂OF₇P₅Ru·PrⁱOH·0.5 CH₂Cl₂: C, 57.57; H, 5.04. Found: C, 57.70; H, 5.00.

[RuF₂(dppp)₂] (3). Compound **1a** (190 mg, 0.175 mmol) and [NMe₄]F (33 mg, 0.35 mmol) were dissolved in CH₂Cl₂ (20 mL). After stirring for 1 day at room temperature, [NMe₄]PF₆ was filtered off and CH₂Cl₂ was removed under vacuum. The residue was dissolved in CH₂Cl₂ (10 mL) and filtered to remove traces of [NMe₄]PF₆. The solution was treated with hexane (20 mL), and the CH₂Cl₂ was evaporated. The resulting light yellow powder was filtered off. Yield: 143 mg (85%). The presence of CH₂Cl₂ and C₆H₁₄ (according to the composition **3**·C₆H₁₄·CH₂Cl₂) was determined by integration of a one-pulse ¹H NMR spectrum. ¹H NMR (CDCl₃): δ 8.0–8.2 (s, br, 4 H, Ph–H), 7.6–7.9 (m, br, 8 H, Ph–H), 6.7–7.6 (m, 28 H, Ph–H), 0.9–2.8 (m, 12 H, P–CH₂). ³¹P NMR (CDCl₃): δ 30.9 (AA'MM'XX', equatorial P, 2 P, J_{A,A'} = –27.2 Hz, J_{A,M} = –32.5 Hz, J_{A,M'} = –35.0 Hz, J_{A,X} = 155.9 Hz, J_{A,X'} = 3.7 Hz), 1.3 (AA'MM'XX', apical P, 2 P, J_{A,M} = –32.5 Hz, J_{A,M'} = –35.0 Hz, J_{M,M'} = 173.9 Hz, J_{M,X} = –16.2 Hz, J_{M,X'} = –24.3 Hz), –143.1 (septet, J_{P,F} = 710 Hz, 1 P, PF₆). ¹⁹F NMR (CDCl₃): δ –341.6 (AA'MM'XX', 2F, Ru–F, J_{A,X} = 155.9 Hz, J_{A,X'} = 3.7 Hz, J_{M,X} = –16.2 Hz, J_{M,X'} = –24.3 Hz, J_{X,X'} = –161.0 Hz). MS (FAB⁺): *m/z* 945 ([M – F]⁺). Anal. Calcd for C₅₅H₅₂OF₇P₅·Ru·C₆H₁₄·CH₂Cl₂: C, 64.55; H, 6.04. Found: C, 64.35; H, 5.89. IR (KBr, cm^{–1}): 443, 414, ν (Ru–F).

X-ray Structures. All X-ray data were collected on a Siemens SMART platform with CCD detector, normal focus molybdenum-target X-ray-tube, graphite monochromator, and ω -scans. Crystal data and refinement details are given in Table 6. Unit cell dimensions determination and data reduction were performed by standard procedures, and an empirical absorption correction (SADABS) was applied. The structures were solved with SHELXS-96 using direct methods and refined by full-matrix least-squares on *F*² with anisotropic displacement parameters for all non-H atoms except disordered atoms,

(41) Lespieau, R.; Wakeman, R. L. *Bull. Soc. Chim. Fr.* **1932**, 51, 384.

Table 6. Crystallographic Data for Complexes 1a, 2a, and 3

| crystal params | 1a | 2a | 3 |
|--|--|--|---|
| empirical formula | C ₅₆ H ₅₆ Cl ₄ F ₇ P ₅ Ru | C ₈₁ H ₇₂ BCl ₄ FOP ₄ Ru | C ₁₁₇ H ₁₂₄ Cl ₆ F ₄ P ₈ Ru ₂ |
| fw | 1268.80 | 1457.95 | 2268.76 |
| cryst syst | monoclinic | monoclinic | triclinic |
| space group (no.) | <i>P</i> 2 ₁ / <i>n</i> | <i>P</i> 2 ₁ / <i>c</i> | <i>P</i> $\bar{1}$ |
| <i>Z</i> | 4 | 4 | 2 |
| <i>a</i> , Å | 11.925(2) | 13.137(2) | 15.819(2) |
| <i>b</i> , Å | 14.798(2) | 34.159(5) | 15.916(2) |
| <i>c</i> , Å | 31.644(5) | 16.989(3) | 22.580(3) |
| α , deg | 90 | 90 | 79.95(3) |
| β , deg | 99.59(2) | 108.03(3) | 71.54(3) |
| γ , deg | 90 | 90 | 89.87(3) |
| volume, Å ³ | 5505.8(14) | 7249.7(19) | 5301.3(14) |
| ρ_{calc} , mg mm ⁻³ | 1.531 | 1.336 | 1.421 |
| μ (Mo K α), mm ⁻¹ | 0.686 | 0.500 | 0.613 |
| <i>F</i> (000) | 2604 | 3008 | 2344 |
| cryst dimens, mm ³ | 0.50 × 0.32 × 0.22 | 0.40 × 0.20 × 0.14 | 0.28 × 0.18 × 0.06 |
| temp, K | 213 | 238 | 293 |
| Measurement of Intensity Data and Refinement Parameters | | | |
| radiation (λ , Å ³) | Mo K α (0.710 73) | | |
| 2 θ range, deg | 1.31–29.94 | 1.19–27.71 | 0.97–26.37 |
| scan type | ω | ω | ω |
| exposure time, s | 10 | 60 | 10 |
| detector dist, mm | 40 | 50 | 40 |
| data colld | –16 ≤ <i>h</i> ≤ 15, 19 ≤ <i>k</i> ≤ 15, –41 ≤ <i>l</i> ≤ 44 | –16 ≤ <i>h</i> ≤ 17, –41 ≤ <i>k</i> ≤ 42, –22 ≤ <i>l</i> ≤ 21 | –19 ≤ <i>h</i> ≤ 15, –19 ≤ <i>k</i> ≤ 13, –28 ≤ <i>l</i> ≤ 25 |
| no. of data colld | 38 839 | 46 464 | 33 385 |
| no. of unique data | 14 217 | 15 150 | 21 391 |
| <i>R</i> _{int} , <i>R</i> _{σ} (%) ^a | 0.0576, 0.0763 | 0.0766, 0.1017 | 0.0541, 0.1330 |
| no. of obs data (<i>I</i> > 2 σ (<i>I</i>)) | 9169 | 9310 | 13 211 |
| no. of params | 668 | 847 | 1222 |
| GOF (<i>F</i> ²) | 1.042 | 1.016 | 0.977 |
| <i>R</i> ₁ (<i>F</i> _o), ^a <i>wR</i> ₂ (<i>F</i> _o ²) ^b | | | |
| obs (%) | 0.0598, 0.1259 | 0.0562, 0.0968 | 0.0610, 0.1300 |
| all (%) | 0.1097, 0.1473 | 0.1186, 0.1187 | 0.1292, 0.1637 |

^a $R_1(F_o) = \sum ||F_o| - |F_c|| / \sum |F_o|$. ^b $wR_2(F_o^2) = [\sum w(F_o^2 - F_c^2)^2 / \sum w(F_o^2)^2]^{1/2}$.

which were refined isotropically. Hydrogen atoms were introduced at calculated positions on nondisordered C atoms and refined with the riding model and individual isotropic thermal parameters. Further details are listed below.

Dark red crystals of **1a** were obtained by slow evaporation of CH₂Cl₂ from concentrated CH₂Cl₂/PrⁱOH solutions of the complex. Analysis of the electron density contour map showed that the fluoride ligand is disordered between two positions (F1A and F1B) and that a small amount of chloride (Cl) is present. Refinement of the occupancy factors *f* of these three atoms with the restraints *f*(F1A) + *f*(F1B) + *f*(Cl) = 1 and *U*(F1A) = *U*(F1B) gave *f*(F1A) = 0.458, *f*(F1B) = 0.396, and *f*(Cl) = 0.146. The latter value was confirmed independently by integration of the ³¹P NMR spectrum of crystals taken from the same batch. Positional and thermal parameters, but not occupancies, were refined in the last cycles. Two CH₂Cl₂ molecules were found, one of which is disordered. Max. and min. difference peaks were +0.969 and –0.894 e Å⁻³; largest and mean Δ/σ were 2.470 and 0.029. Colorless crystals of **2a**BPh₄ were obtained by slow evaporation of CH₂Cl₂ from a solution of **2a**PF₆ (5 mg, 5 μ mol) and NaBPh₄ (20 mg, 0.6 mmol) in CH₂Cl₂/PrⁱOH (6 mL). Max. and min. difference peaks were 0.727 and –0.818 e Å⁻³; largest and mean were Δ/σ = 0.006 and –0.129.

A yellow crystal of **3**, obtained by slow evaporation of CH₂Cl₂/hexane solutions, was mounted in a 0.3 mm glass capillary, which was sealed to prevent loss of solvent of crystallization. Besides two crystallographically independent [RuF₂(dppp)] molecules, four sites are occupied by cocrystallized solvent: site 1 contains CH₂Cl₂ (not disordered), sites 2 and 3 contain CH₂Cl₂ or hexane (0.5:0.5 occupancy), and site 4 contains CH₂Cl₂ (disordered over three positions). The resulting content of the unit cell is **3**·1.5 CH₂Cl₂·0.5 C₆H₁₄, in reasonable agreement

with analytic and ¹H NMR data. Positional and thermal parameters and occupancies of disordered molecules were refined with constrained C–C (1.54 Å) and C–Cl (1.74 Å) bond lengths. Max. and min. difference peaks were 1.732 and –0.869 e Å⁻³; largest and mean Δ/σ were 0.001 and –0.11.

Reaction of 1a with R–X. A typical procedure is as follows. Complex **1a** (22 mg, 20 μ mol) and the corresponding substrate **5a–e** (20 μ mol) were dissolved in CDCl₃ (0.4 mL) in an NMR tube fitted with a Teflon liner and a Young valve. All manipulations were performed under purified nitrogen in a glovebox (Braun). The reaction was monitored by ¹H, ³¹P, and ¹⁹F NMR spectroscopy. The identity of the fluorinated products was determined by ¹⁹F NMR spectroscopy by comparison with literature data.^{20,35–38} In the case of reactions with **5a** and **5b**, integration of the gate-decoupled ¹⁹F NMR spectrum of the reaction mixture (taking the [PF₆][–] signal as reference) indicates quantitative conversion to the fluorinated product **6**. For reactions with **5a** (additionally to ¹⁹F NMR), **5c**, and **5d**, the product distribution was determined by integration of the ¹H NMR spectrum using an appropriate ¹H NMR signal of the complexes (δ 7.9–7.7, 4 H, Ph*H*) as internal standard and is based on (converted) **5a–d**.

Relevant features of ¹H and ¹⁹F NMR spectra of the reaction solutions are given below. Reaction with **5a**: ¹H NMR (CDCl₃): δ 5.22 (s, 1 H, CBr–*H*, **5a**), 6.02 (s, 1 H, CF–*H*, **6a**); ¹⁹F NMR (CDCl₃): δ –165.4 (d × d × d, 1F, *J*_{F,H} = 47.5, 11.7, 1.0 Hz, C–*F*, **6a**).²⁰ Reaction with **5b**: ¹⁹F NMR (CDCl₃): –126.1 (lit. –126.2,³⁵ s, 1 F, C–*F*, **6b**). Reaction with **5c**: ¹H NMR (CDCl₃): δ 6.31 (s, 1 H, CBr–*H*, **5c**, 30%), 6.48 (d, 1 H, *J*_{F,H} = 47.8 Hz, Ph₂C(F)–*H* (**6c**), 70%), 5.40 (lit. 5.38,³⁹ s, 1 H,

$\text{Ph}_2\text{CHOC}(H)\text{Ph}_2$, traces). ^{19}F NMR (CDCl_3): δ -166.9 (lit. -169,³⁶ d, 1 F, $J_{\text{F,H}} = 46.6$ Hz, lit. 48,³⁶ $\text{Ph}_2\text{C}(\text{H})-F$, **6c**). Reaction with **5d**: ^1H NMR (CDCl_3): δ 1.83 (s, 9 H, $\text{C}(\text{CH}_3)_3$, **5d**, 50%), 1.38 (lit. 1.30,³⁸ d, 9 H, $J_{\text{F,H}} = 21.1$ Hz, lit. 20,³⁸ $\text{F}-\text{C}(\text{CH}_3)_3$ (**6d**), 10%), 4.66 (lit. 4.55,⁴² m, 2 H, $(\text{CH}_3)\text{C}=\text{CH}_2$, 38%), 1.75 (t, 6 H, $J_{\text{H,H}} = 1$ Hz, $(\text{CH}_3)\text{C}=\text{CH}_2$, 38%), 1.28 (lit. 1.27,⁴⁰ s, $(\text{CH}_3)_3\text{CO}(\text{CH}_3)_3$, 2%). ^{19}F NMR (CDCl_3): δ -131.0 (lit. -132,³⁶ 10 lines, 1 F, $J_{\text{F,H}} = 21.1$ Hz, lit. 21,³⁶ $\text{C}-F$, **6d**).

Acknowledgment. Financial Support from the Swiss National Science Foundation and the ETH Zürich is gratefully acknowledged.

Supporting Information Available: Details of X-ray analyses. This material is available free of charge via the Internet at <http://pubs.acs.org>.
OM0000156